AFE BABALOLA UNIVERSITY

JULIUS-ABUDA BONNITTA OKHASOMINUNO

14/ENG01/011

MEASURMENT OF GAS VOID FRACTION IN HORIZONTAL PIPE

AFE BABALOLA UNIVERSITY ADO-EKITI (ABUAD)

TECHNICAL REPORT WRITING

ACADEMIC YEAR: 2017-2018

DR YAHAYA

ABSTRACT

This experiment presents an experimental study of void fraction distribution in large diameter horizontal pipe flow. A double conical hot film probe has been designed to measure simultaneously the void fraction and the bubble velocity. Measured void fractions were calibrated in a 2-in. diameter pipe with bubble flow. Tests have been carried out along the pipe axis and in both cross-sectional planes. Fully developed flow is identified at a distance more than 100times pipe diameter from the mixer. Void measurements in the large diameter horizontal pipe are comparable with results in a 1.0-in. diameter horizontal pipe.

Two new sets of correlations are discussed in this study. The first predicts the longitudinal distribution of void fraction, where correlations are expressed in terms of axial location and flow volumetric quality. In the second, distribution of the void fraction profiles are found to be almost flat in the radial/horizontal plane for which power law may be assumed.

Acknowledgements

We appreciate the support provided by the mechanical workshop at the Department of Physics, University of Bergen in design advice and the supply of equipment for these experiments. This work has been funded by the Research Council of Norway.

Table of Contents

List of figures

List of table

List of equations

1 Measurement of Gas Void fraction in Horizontal Pipe

1.1 Introduction

The oil and gas production industry has a need for accurate measurements of the oil and gas fractions in pipelines. Improved production techniques have made it economically feasible to produce from smaller (marginal) reservoirs by using subsea and even down- hole production units. With several production lines running into a production separator on the platform, it is impossible to measure the gas fraction in each line. At present, the flow is separated and then the fractions are measured. A test separator is used to separate the flow and then the individual phases in each production line are measured at intervals. Usually, turbine meters and orifice plates are used to measure the oil and gas flows, respectively. One disadvantage of this technique is that test separators are large units and space costs on a production platform are high.

A multiphase meter on each line that measures the water, oil and gas flows offers better production control than test separators, and online measurements of production at each unit are necessary to optimize production. During the past decade, much work has been devoted to the development of three-phase meters cap- able of measuring oil, gas and water in pipelines. Multi- phase meters should preferably have non-intrusive sensors for several reasons, including the elimination of pressure drop over the instrument, their lack of impact on the flow and the elimination of detector corrosion. Most multiphase meters include measurements of either single- or multi-energy gamma-ray attenuation for fraction measurements (1).

Conventional gamma-ray densitometers utilize a single ^{137}Cs (662 keV) source and detector (*P*hoto *M*ulti- plier *T*ube, PMT) located diametrically opposite each other. PMTs have a diameter of several centimeters. Gamma-ray densitometers have clamp-on capability, which is to say that these instruments can be installed and removed without shutting down the process. Where low-energy gamma-ray densitometers are used, the clamp-on capability is lost due to the need for radiation windows in the pipe walls. However, gamma-ray densitometers used in multiphase meters do not need to be clamp-on.

2 Gamma-ray densitometers

In two-component flows in which the components have sufficiently different densities, such as oil-gas mixtures, gamma densitometers can be used to measure the volume fractions, e.g. the gas fraction of the flow components. The *void fraction* is defined as the gas volume fraction divided by the total volume of the flow. Only two-phase flows are studied in this work. Measurements of gas fractions are generally dependent on the internal distribution of the components inside the pipe- line, i.e. on the flow regime. Figure 1 shows typical two- phase flow regimes for vertical and horizontal flows.

Figure 1shows that there are three basic flow regimes. These are homogeneous flows (bubble flow in vertical and dispersed bubble flow in horizontal), annular flows, and stratified flows. The other flow regimes are essentially combinations of these basic flow regimes with periodicity. Several efforts have been made to design flow homogenizers to mix the flow components (2), and commercial multi-phase meters with mixers are available. The advantage of mixers is that single-beam gamma-ray densitometers provide accurate measurements independent of the original flow regime. A disadvantage is the pressure drop, and for pipes where non- intrusive instruments are required other methods have to be considered. Any information about the flow regime is lost when mixers are utilized. In instruments without mixers, knowledge of the flow regimes has been used to obtain more reliable measurements of the void fraction. For instance, vertical upstream stratified flows will never occur.

The most common measurement configuration for single-beam gamma densitometers is shown in Figure 2. The void fraction is determined by measuring the average effective linear attenuation coefficient in the measurement volume over the cross-section of the pipe. The results obtained by using these single-beam densitometer depend on the flow regime, since the measurement cross-section volume normally is less than that covered by the pipe cross-section (3).

The true void fraction is the gas volume fraction of the total flow volume of the cross-section. The calculated void fraction is the gas fraction in the volume defined by the radiation beam and detector area, i.e. the measurement volume (see Figure 2). By comparing the true void fraction and the calculated void fraction, the accuracy of the measurements for different flow regimes can be obtained.

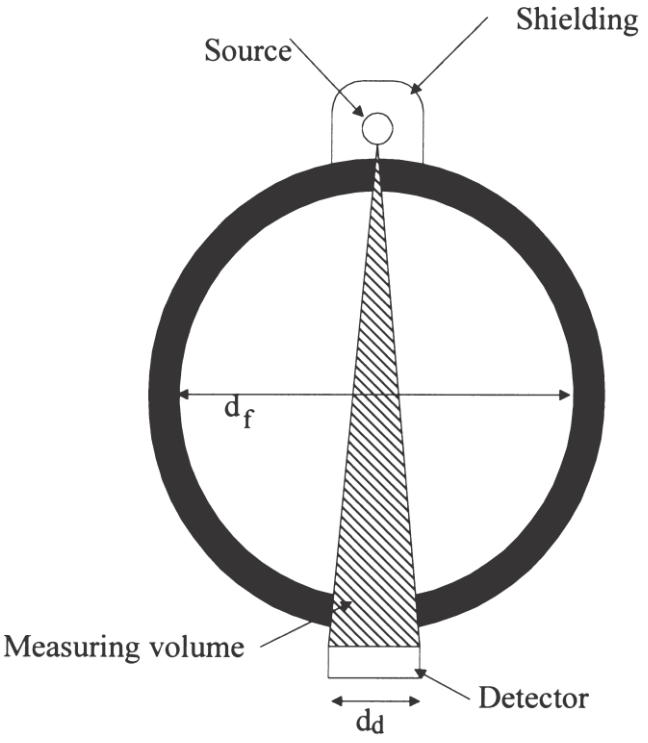

Figure 1: Single-beam gamma densitometer with point source and detector located diametrically opposite each other.

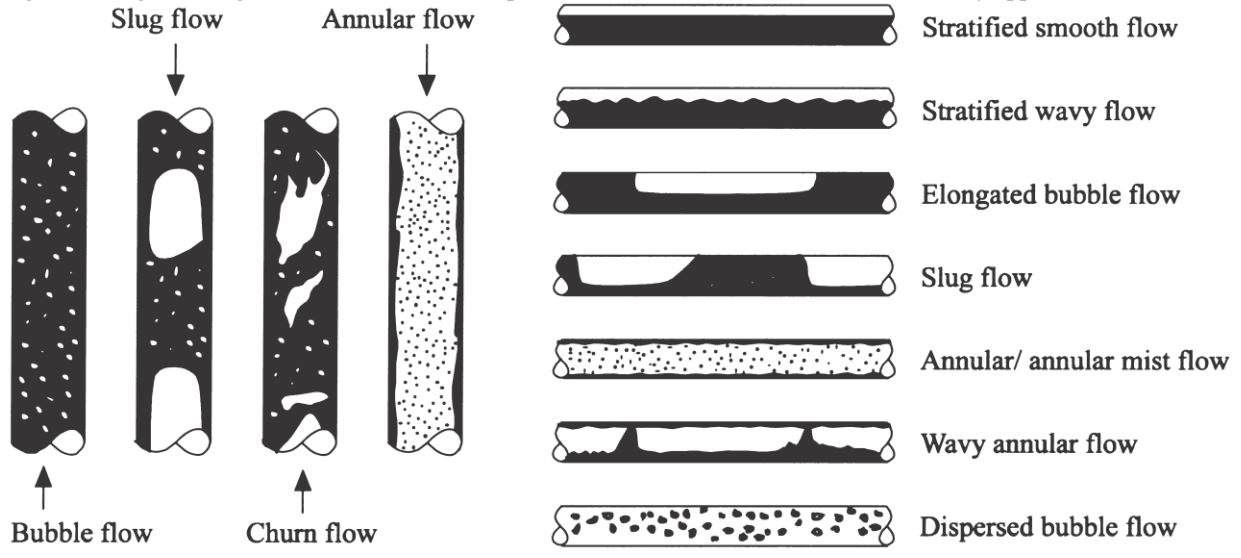

Figure 2: Typical flow regimes for vertical and horizontal flows. Black and white areas represent liquid and gas, respectively

Where R is the total radius of the flow and r_0 is the radius of the gas core. Similarly, an expression of the void fraction in the measured volume of annular flows with a parallel radiation beam can be found as follows:

3 Flow regime dependence of single-beam gamma densitometers

Only idealized flow regimes have been considered in this paper in order to simplify the calculations and to simplify the fabrications of the phantoms. Then, the ideal flow regimes eliminate any differences between the calculations and the phantoms used in the measurements. It can been seen from Figure 3 that the measurement volume depends on the detector area and collimation of the gamma-ray beam. The detector area thus influences sensitivity to the flow regime. In homogeneous flows the linear attenuation coefficient is similar over the entire cross-section. Measuring the linear attenuation coefficient at a single position provides sufficient information about the void fraction of the flow.

When the detector diameter is much smaller than the flow diameter (a narrow fan beam), the diameters of the areas defined by the beam and flow, d_1 and d_2, are assumed to be plane and parallel to the detector plane d as shown in Figure 3. Furthermore, it is assumed the pipe wall is thin compared to the flow diameter, $2R$. Thus, the measurement volume can be defined as a cone in the flow, as shown in Figure 3. To simplify, perfect pipe axis symmetry is assumed, so the flow is symmetrical.

On the basis of the geometry illustrated in Fig. 3, the void fraction in the sensitive volume of annular flows

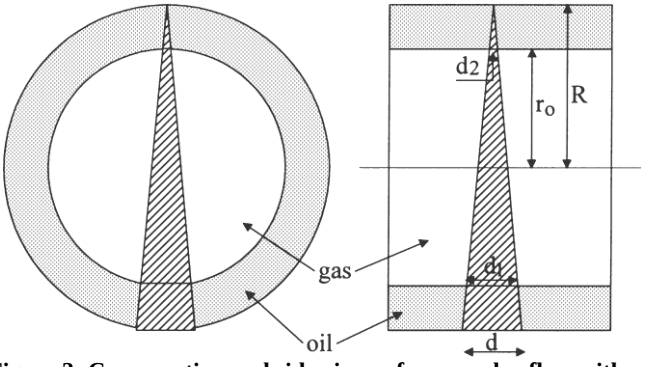

Figure 3: Cross-section and side views of an annular flow with a narrow fan radiation beam.

with a narrow fan radiation beam can be expressed as follows:

ac 5 4R3 •(3R2 1 r02) Equation 1

where R is the total radius of the flow and r_0 is the radius of the gas core. Similarly, an expression of the void fraction in the measured volume of annular flows with a parallel radiation beam can be found as follows:

a 5 0 Equation 2

c R

From Fig. 3 it is evident that the true void fraction of an annular flow is calculated by:

a_t 5 p·R^2·d 5 R^2 Equation 3

By studying Eqs. (1)–(3), it can be seen that for $r_0 = 0$ and $r_0 = R$ the calculated void fraction, a_c, and the true void fraction, a_t, are identical. However, within these limits, the calculated void fractions in annular flows with a narrow fan radiation beam are functions of r_0^3/r^3 while for a parallel radiation beam the calculated void fraction is a function of r_0 and the true void fraction is a function of r_0^2. Obviously, measurements of the void fraction of annular flows are independent of the direction of the source–detector axis because of the symmetry of annular flows.

In Figure 4 the calculated void fraction, a_c, is plotted

Fig. 4. Deviation between calculated and true void fractions of annular flow for narrow fan and parallel radiation beam. The solid line represents the ideal case with no deviation between true and measured void fraction deviation is observed between measured and true void fractions.

In Fig. 8 the calculated void fraction, a_C, is plotted against the true void fraction, a_t, for stratified flows with top–bottom configuration. The deviation between the calculated and true void fractions is at a minimum with

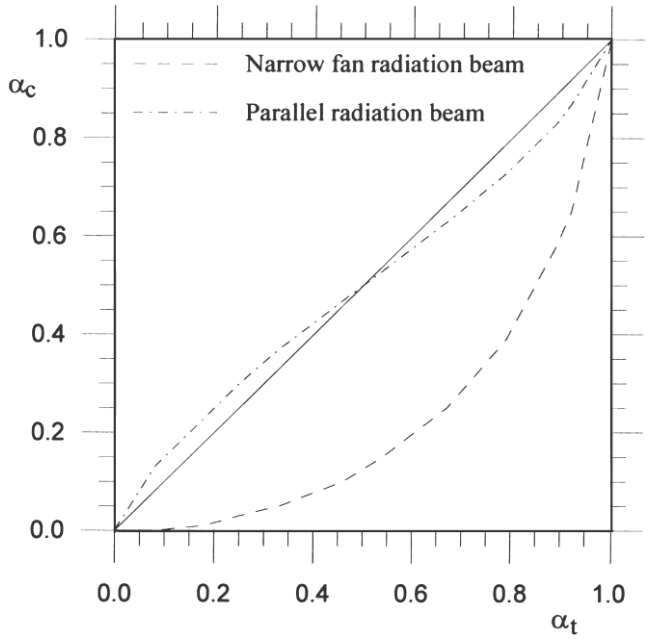

Figure 4: Deviation between measured and true void fraction of stratified flow for narrow fan beam. The solid line represents the ideal case with no deviation between true and measured void fractions.

versus the true void fractions, a_t, with narrow fan and parallel radiation beams. There are no deviations between the calculated void fractions and the true void fraction when the flow is single phase, since the flow in the measured volume represents the flow over the entire cross-section. The maximum deviations appear when the true void fraction is between 0.1 and 0.6. Fig. 4 shows that calculated void fractions in annular flows are over- estimated, and that the narrow fan radiation beam gives a lower deviation than the parallel radiation beam.

In the same way as with annular flows, simplifications have been made with stratified flows, i.e. a much smaller detector diameter compared with the pipe diameter, and a thin pipe wall. The sensitive volume will then be as shown in Fig. 5. The lack of pipe-axis symmetry of stratified flows produces measurements of the void fraction that depend on the direction of the source–detector axis. In what follows, the direction will be called *top– bottom configuration* when the source is above and the detector is below the oil–gas interface, as shown in Fig.5. When the detector is above and the source is below the oil–gas interface the direction will be called *bottom*– figuration is turned 90°, the direction will be called *side-by-side configuration.*

For top–bottom configuration and stratified flows, the calculated void fraction in the measurement volume with a narrow fan radiation beam can be written as:

$$a_c = \frac{(2R - L_0)^3}{8R^3} \quad \textbf{Equation 4}$$

where L_0 is the level of oil.

With bottom–top configuration the gas volume will not be equal to that of top–bottom configuration, and for bottom–top configuration the calculated void fraction of the measurement volume can be expressed as:

$$a_c = \frac{(2R - L_0)^2}{8R^3} \cdot (L_0 + 2R \cdot L_0 + 4R^2) \quad \textbf{Equation 5}$$

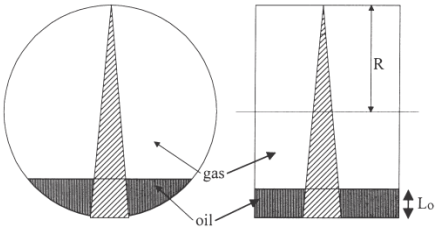

Figure 5: Cross-sectional and side views of stratified flow with narrow fan radiation beam

The calculated void fraction of stratified flows with parallel beams can be found as:

$$a_c = \frac{L_0}{2R} \quad \textbf{Equation 6}$$

With parallel beams there are no differences between the top–bottom and bottom–top configurations, and the side-by-side configuration will appear to be identical to that of the side-by-side configuration with narrow fan beams, shown in Fig. 7.

For side-by-side configurations the calculated void fraction will be 1 and 0 for oil levels lower and higher than the detector, respectively. Due to the small detector diameter compared with the flow diameter, i.e. a small measurement volume, this side-by-side configuration will be highly sensitive to changes in oil level when this covers some of the measurement volume, as shown in Fig. 7.

Based on Fig. 6, it can be shown that the true void fraction of stratified flows can be found by [3]:

$$a_t = 1 - \frac{1}{\pi}\left[\arccos\left(\frac{R - L_0}{R}\right)\right] \quad \textbf{Equation 7}$$

On the basis of Eqs. (4), (5) and (7) the deviations between the calculated void fractions and the total void fraction for stratified flows with different source–detec- tor directions are plotted in Fig. 7.

By inserting $L_0 = 2R$ and $L_0 = 0$ into Eqs. (4), (6) and (7), the calculated void fractions and the true void fraction are 0 and 1, respectively. When flows consist of only one component, it is obvious that the density, or more correctly, the linear attenuation coefficient, is equal over the entire cross-section of the flow. Therefore, no

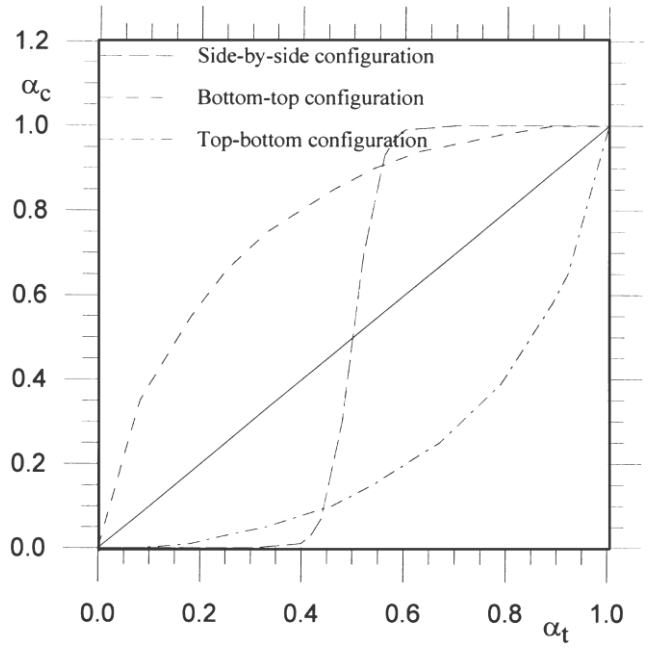

Figure 6: Deviation between measured and true void fraction of stratified flow with narrow fan beam with different source-detector orientations. The solid line represents the ideal case with no deviation between true and calculated void fractions.

deviation is observed between measured and true void fractions.

In Fig. 8 the calculated void fraction, a_c, is plotted against the true void fraction, a_t, for stratified flows with top–bottom configuration. The deviation between the calculated and true void fractions is at a minimum with

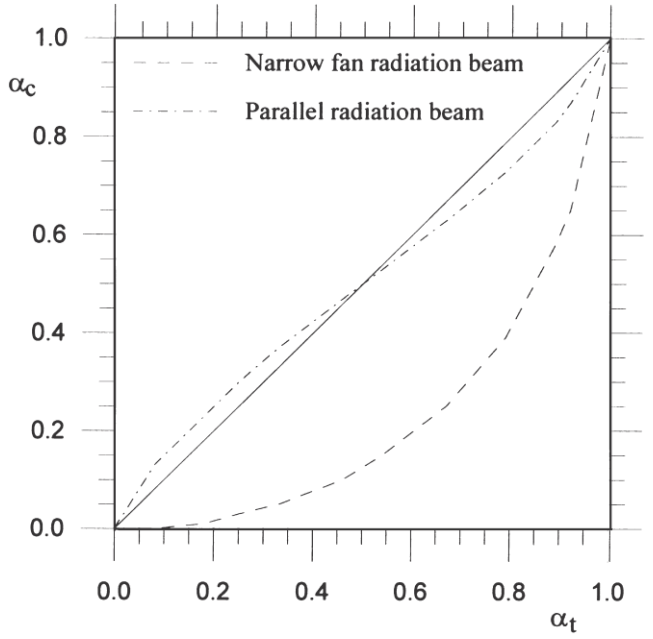

Figure 7: Deviation between measured and true void fraction of stratified flow for narrow fan beam. The solid line represents the ideal case with no deviation between true and measured void fractions.

parallel beams and reaches a maximum with narrow fan beams. In contrast to annular flows, the calculated void fraction of top–bottom configured stratified flows is underestimated.

By comparing Figs. 4 and 8, we can see that the accuracy of void fraction measurements is highly dependent on the flow regime and the radiation beam. For this reason, in order to obtain accurate void fraction measurements, the flow regime must be taken into account.

4 Multi-beam gamma-ray measurement principles

Low-energy sources such as ^{241}Am (59.5 keV) offer the possibility of a compact design as a result of low shielding requirements (2 mm of lead). Furthermore, the use of compact semiconductor detectors such as cadmium zinc telluride (CZT) detectors, allows multi-beam configurations which represent flow cross-section better than single-beam gamma-ray densitometry. In addition, thanks to the compactness of the source and detectors, low-energy gamma-ray densitometers can be integrated into the pipe wall, as shown in Figure 8.

The predominant mechanisms of interaction for low- energy photons are the photoelectric effect and Compton scattering. Their probabilities of interaction depend on the atomic number of the absorber. The relationship is approximately linear for Compton scattering, which is to say that the interaction probability is directly proportional to the density of the absorber. For the photo- electric effect the interaction probability is proportional to the atomic number to the power of 4–5.

Photon scattering is often regarded as an undesirable effect in gamma-ray attenuation measurements since it complicates the interpretation of the results. Build-up, i.e. the extra contribution to transmission measurements

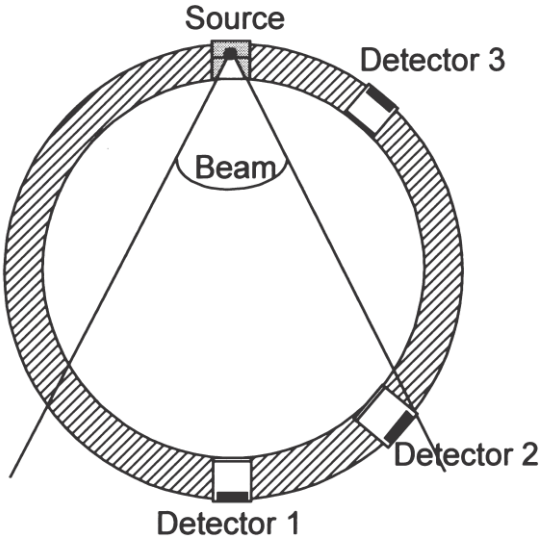

Figure 8: Compact low-energy multi-beam gamma-ray densitometer.

from scattered radiation, has to be considered, particularly if wide-beam measurement configurations are used (3). In fluid flow fraction measurements, however, it is possible to take advantage of this effect since it effectively means that the gas–liquid distribution outside the geometrical volume defined by the source and the detector affects the measurement result (5). This may to some extent be regarded as a geometrical measurement averaging over the pipe cross-section, especially for backscattered radiation where there is no contribution from transmission. A Monte Carlo simulation model has been developed and implemented in order to study trans- mitted and scattered photons over the pipe cross-section (4).

Measuring the spectral detector response at several positions around the pipe allows the transmitted and scattered photons to be detected in several positions. Pulse height analysis (PHA) is used to study the energy depositions in the detectors. Once the detector responses have been combined and utilized, the void fraction and flow regime can be determined. A suitable method, as used here, of examining single- and multi-beam gamma- ray densitometry configurations, is to use phantoms made of polypropylene and compare the data from the detector responses with a range of flow regimes and void fractions.

5 Experimental setup and results

In this work, an aluminum pipe was made to test the multi-beam gamma-ray measurement principles. Instead of oil, phantoms of polypropylene (density 0.91 g/cm^3) were employed. Such phantoms are necessary to obtain reliable reference values. The density of the phantoms is higher than that of most oils, but is close enough to verify the principle. The inner and outer diameters of the pipe are 80 mm and 90 mm, respectively. A ^{241}Am (59.5 keV) source

and a single eV A1361 CZT (CdZnTe) semiconductor detector were used in the experiments, in addition to a eV-550 preamplifier, a Tennelec TC244 amplifier and an Oxford PHA.

Using the phantoms, static measurements were performed. That means both the void fraction and flow regime were constant during the measurements, giving reliable references. A complete measurement series of one phantom consisted of detector responses from 17 positions around the pipe to represent the detector positions from 180° (diametrical position) to 52°.

In a system in which measurement values vary rap- idly, the measurement time (integration time) plays an important role, since measurement time and statistical error are closely related. Longer measurement times give lower statistical errors and vice versa. Fluctuations in measurement values will be smoothed out with a longer measurement time. It is important to use low Z-number pipe wall materials with low-energy gamma-ray densitometers in order to minimize beam attenuation in the walls. Suitable pipe wall materials include aluminum, titanium or plastics. Windows can be made of these materials rather than using them for the whole pipeline. In order to obtain short measurement times, the pipe wall material and the source activity must be chosen care- fully. In our experiments, a 14 mCi ^{241}Am source and a measurement time of 600 s were chosen because of the static nature of the experiment. In a real dynamic system a ^{241}Am source with higher activity and a shorter measurement time would have to be considered. The statistical error is inversely proportional to the square root of number of counts, thus a smaller measurement time will increase the statistical error. For instance, use of a 300 mCi source and a measurement time of 1s will decrease the number of counts by 30, thus the statistical error will be increased by about 5.4 times.

The aluminum pipe, source and detector are mounted in a computer-controlled test platform, on which the detectors are positioned around the pipe to an accuracy of 6 1° (6). The CZT detector is moved by 8° between each measurement to obtain detector responses in several positions around the pipe with fixed flow regimes. As shown in Table 1, various polypropylene phantoms are used to simulate flow regimes and void fractions.

More information is obtained with multi-beam densitometry than with single-beam gamma-ray densitometry. Void fraction measurements of the same pipe and phantoms from single-beam and multi-beam low-energy gamma-ray configurations have been compared in order to study their performance.

The principle of single-beam gamma-ray densitometers is based on the concept of expressing the void fraction in terms of transmitted intensity, which is the number of photons detected in the full energy peak in the measurement time period. This means counting pho- tons with energy higher than a given threshold value, which was 40 keV in our experiments. The void fraction can be found as:

Table 1

Void fraction and flow regime phantoms made for the experiment

Void fraction (%)	Flow regime phantom
0	Homogeneous
20	Stratified
20	Annular
25	Annular
50	Annular
50	Stratified
56	Annular
70	Annular
80	Stratified
100	Homogeneous

$$a = \frac{\ln\left(\frac{I_{mix}}{I_{oil}}\right)}{\ln\left(\frac{I_{gas}}{I_{oil}}\right)}$$ **Equation 8**

where I_{oil} and I_{gas} correspond to 100% oil and 100% gas, respectively. These values are used as calibration values.I_{mix} is the measured intensity which depends on the amount of oil and gas in the flow Figure 8 assumes that the contribution of scattered photons detected is negligible. The contribution of scattered photons depends on several

parameters, including pipe wall material and thickness, void fraction (i.e. linear attenuation coefficient), distribution of oil and gas in the pipe (i.e. flow regime) and the presence of a detector collimator.
During the calibration process scattered photons are included in the calibration values.

The performance of single-beam gamma-ray densitometry can be studied with the aid of the phantoms listed in Table 1, which have fixed void fractions and flow regimes. A PMT is located diametrically opposite the source (^{241}Am). In Figure 10 the measured void fractions of these known phantoms of the single-beam gamma- ray densitometer are presented. A steel cap with a Ø10 mm hole was used to collimate the PMT in order to minimize the contribution of scattered photons and to achieve a lower count rate. The deviation between the true void fraction and the measured void fraction appears

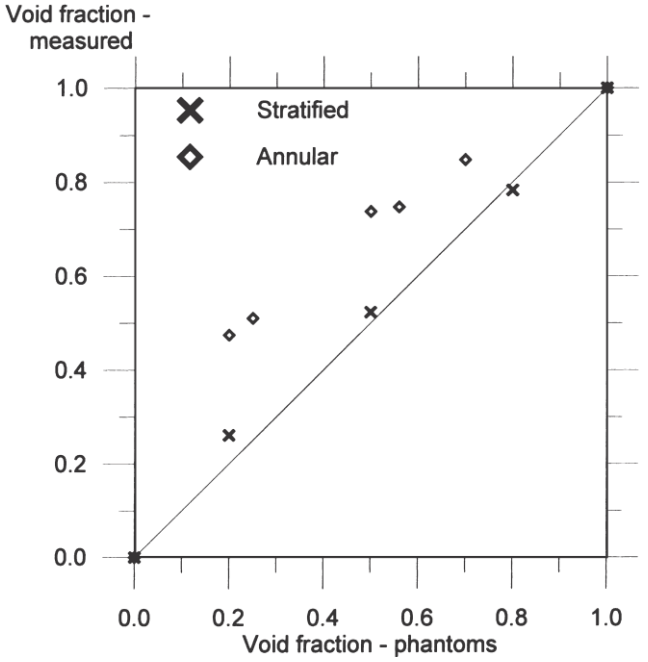

Figure 9: Measured void fraction versus true void fraction using single-beam gamma-ray densitometer with 241Am source. The solid line represents the ideal case, with no deviation between true and measured void fractions.

to be largest with annular flow regime phantoms, Figure 9.

By comparing the measured void fractions in Fig. 10 with the calculated void fractions in Figs. 4 and 8, it can be seen that measured void fractions appear to be equal to calculated void fractions for parallel beams. The flow regimes are the cause of the deviations between measured and true void fractions. Since the deviations appear to be similar for calculated and measured void fractions, the models used to describe the calculated void fraction of annular and stratified flows are satisfactory.

A performance study of the multi-beam gamma-ray measurement principle requires measurements obtained by a conventional gamma-densitometer. Such a densitometer was constructed: it consists of a single collimated 1 mCi ^{137}Cs (661.7 keV) source and one 2ⅈ PMT, installed on a 90 mm steel pipe with a wall thickness of 5 mm.

The phantoms shown in Table 1 were used, as they had well-defined void fractions. In accordance with Eq. (8), the measured void fractions were found on the basis of the measured intensities for different void fractions and flow regimes. Fig. 11 plots the measured void fractions against the true void fractions. By comparing the experimental data from the conventional gamma-densitometer with the data in Figs. 4 and 8, it can be seen that the data fit fairly well with the annular and stratified flows with parallel radiation beams, respectively.

It is obvious from Eq. (8) that the I_{gas}/I_{oil} ratio expresses the sensitivity of the system. It can be seen that

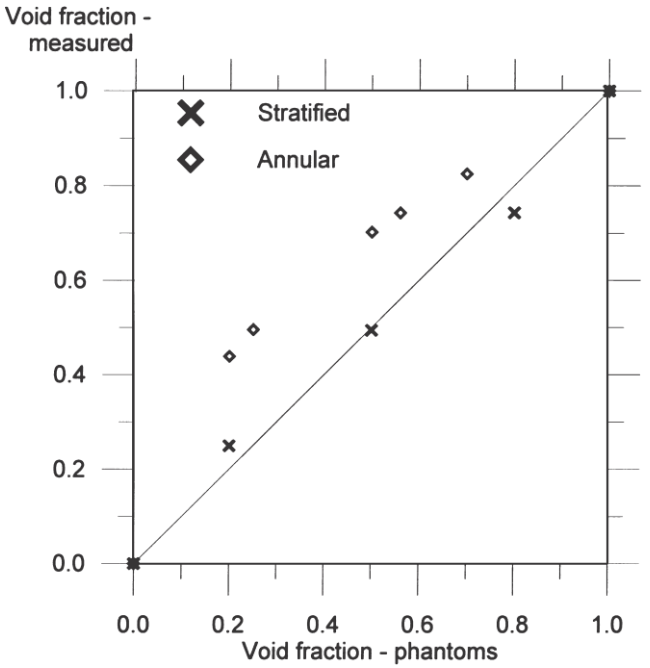

Figure 10: Measured void fraction versus true void fraction using conventional gamma-ray densitometer with 137Cs source. The solid line represents the ideal case with no deviation between true and measured void fractions.

this ratio is higher than 1 in detectors that are registering transmitted photons, i.e. in the collimated beam (see Figure 10and Fig. 13). In multi-beam gamma-ray densitometry the I_{gas}/I_{oil} ratio is smaller than 1 outside the beam. This means that in the oil–gas mixture the number of scattered photons decreases as void fraction increases, due

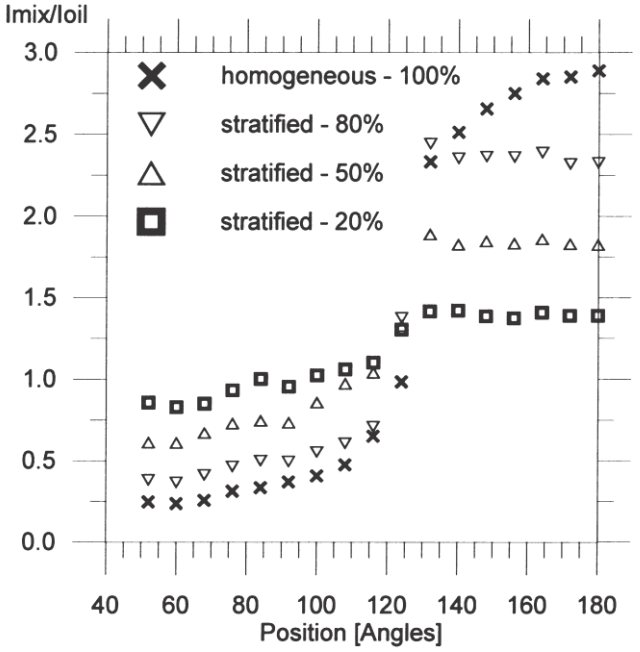

Figure 11: Imix/Ioil ratios plotted versus detector position for stratified flow phantoms.

to the lower probability of interactions in the gas. Since the I_{gas}/I_{oil} ratio is fixed for a given gamma-ray densitometer, the deviations between the real and measured void fraction must be found in the I_{mix}/I_{oil} ratios.

Figs. 12 and 13 plot the I_{mix}/I_{oil} ratios for all the phantoms. The ratios are found by counting the number of events with constant measurement time in the full energy peak. By comparing Figs. 12 and 13 it can be seen that the I_{mix}/I_{oil} ratios are 1.3–1.4 for stratified flow phantoms and are close to 1 for the annular flow phantoms at the detector position of 124°. This means that at this detector position, the system will only be sensitive to the stratified flow phantoms. It can also be seen that the I_{mix}/I_{oil} ratios of stratified flow phantoms are flat over the detector positions covered by the beam. This is due to the fact that the transmitted beam has a shorter path through the stratified phantoms at angles smaller

than 180°, com- pared with its path through annular flow phantoms. This suggests that the I_{mix}/I_{oil} ratios of two detectors located in the beam could be used to detect whether the flow regime is stratified or not. It should be noted that the value of I_{mix}/I_{oil} ratios versus detector position depends on the distribution of the photon emission from the source.

Using the data shown in Figs. 12 and 13, the void fraction can be calculated according to Figure 8. The measured void fractions at 180° appear to be similar to the data obtained by the PMT (Fig. 10). In this position the measured void fractions with stratified flow phantoms are close to the true void fractions.

It was discovered experimentally that several detector positions underestimated the void fraction of stratified and annular flow phantoms. By taking these void fractions into account, the dependency of the flow regime can be reduced. The measured void fraction based on the experimental data of stratified and annular flow phantoms from four detector positions were used to calculate the mean value of the void fraction. The mean values of the void fractions were compared to the true void fractions. Based on the detector positions giving the mean void fractions closed to the true void fractions, the detector positions were selected.

In Figure 13 the void fractions based on the experimental data obtained using the phantoms are plotted for detector positions at 180°, 140°, 68° and 52°. Only scattered pho- tons are detected in the detector positions at 68° and 52°. At 68° and 52°, however, it can be seen that void fraction measurements of the annular flow phantoms are under- estimated and are closer to the true void fraction than measurements made at 180°. It is interesting to note at 68° and 52°, the measurements of annular flow phantoms are closer to the true void fraction than measurements of stratified flow phantoms.

Fig. 14 and Fig. 15 suggest that the data are distributed more or less equally around the solid line, which

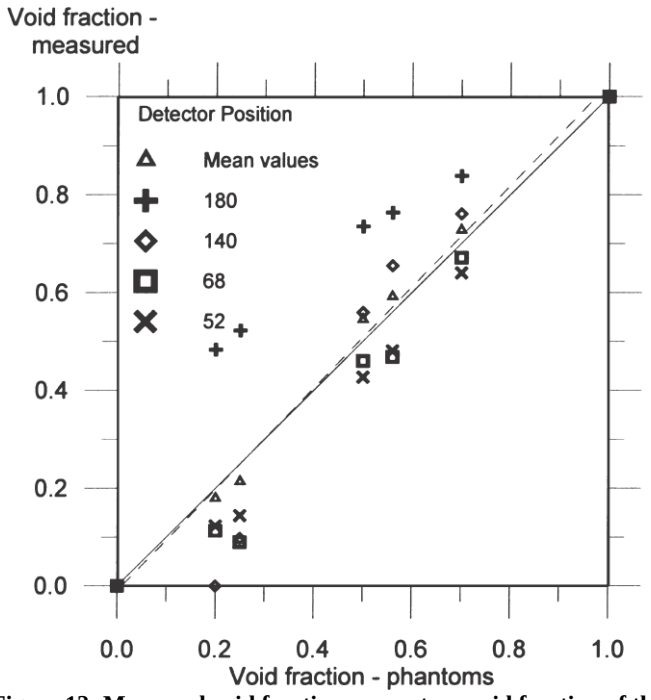

Figure 12: Measured void fraction versus true void fraction of the annular phantoms at several detector positions. The solid line represents the ideal case with no deviation between true and measured void fractions. The dashed line is the best curve fit of the mean values.

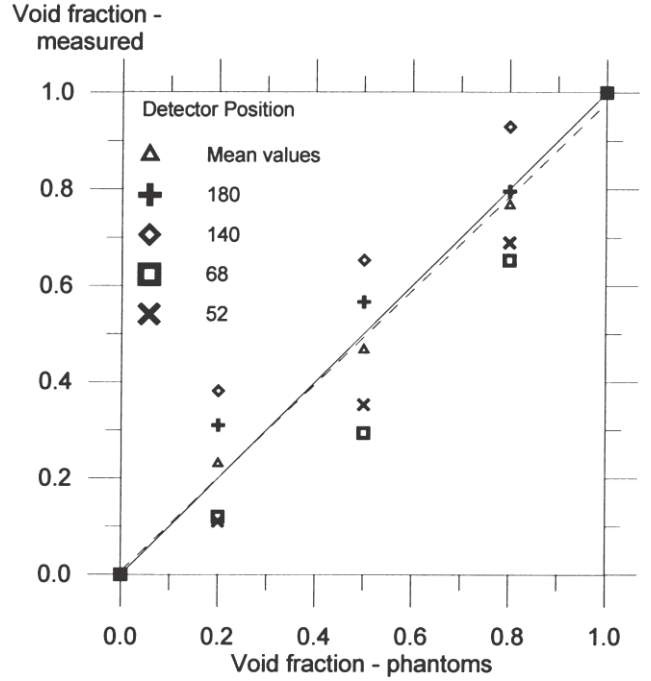

Figure 13: Measured void fraction versus true void fraction of the stratified phantoms at several detector positions. The solid line represents the ideal case with no deviation between true and measured void fractions. The dashed line is the best curve fit of the mean values.

indicates that there was no deviation between measured and true void fraction. This means the mean values of the measured void fractions of the selected detector positions are close to the true void fractions. A curve fitting of the mean values gives a curve very close to the true void fraction of the phantoms, as shown in Fig. 14 and Fig. 15.

Around the pipe, the minimum number of counts in the full energy peak will be at detector positions outside the beam and when the void fraction is 1, due to the low probability of interaction in gas. The most important

contribution to the total statistical error of the measured void fraction is made by positions with the lowest number of counts. The relative standard deviations due to the number of counts in detector positions 52° and 68° are 0.30% and 0.32%, respectively. This suggests that statistical fluctuations in the measured void fractions are negligible, and that the distributions of the data in Figs. 14 and 15 are caused by the different probabilities of scattered photons to reaching a given detector position with different phantoms.

6 Conclusions

The performance of single-beam and multi-beam gamma-ray densitometry has been examined. It has been shown how the sensitivity of single-beam densitometers is related to the flow regime and the beam. With conventional technology, the sizes of PMT and shielding are an obstacle to obtaining a compact multi-beam densitometer. The low-energy multi-beam gamma-ray densitometry discussed in this paper is investigated by one single source and one CZT semiconductor detector. Several measurements are performed around the pipe on the same cross-section, representing several detectors installed. Due to the low energy of the source, shielding requirements are reduced, with the result that the source and detectors can be integrated into the pipe-wall.

Using the multi-beam gamma-ray measurement principles, it has been shown that accurate measurements can be made when measurements of four detector positions around the pipe are combined. However, it should be noted that the results depend on the pipe-wall material and thickness, pipe dimensions, and finally, on the com- position of the flow.

References

[1] R. Thorn, G.A. Johansen, E. Hammer, Recent developments in three-phase flow measurements, Meas Sci Tech 8 (1997) 691–701.

[2] P.S. Harrison, G.F. Hewitt, S.J. Parry, G.L. Shires. Development and testing of the "Mixmeter" multiphase flow meter. Proceedings of North Sea Flow Measurement Workshop, 1995.

[3] H. Linga. Measurements of two-phase flow details. Drang. Thesis, Norwegian Institute of Technology, University of Trondheim,1991.

[4] E. Åbro, G.A. Johansen, H. Opedal. A radiation transport model as a design tool for gamma densitometers. Submitted for publi- cation, 1998.

[5] H. Opedal. Integrated gamma densitometer and venturi meter for liquid phase measurements. M.Sc thesis, University of Bergen, 1997 (in Norwegian).

[6] G.A. Johansen, T. Frøystein, H. Pedersen, B. McKibben. A flexible test platform for investigating gamma-ray tomography geometries and applications. Proceedings of Frontiers in Industrial Process Tomography II, Delft (Netherlands), 9–12 April, 1997